Competition between strain-induced and temperature-controlled nucleation of InAs/GaAs quantum dots

P. Howe, E. C. Le Ru, E. Clarke, B. Abbey, R. Murray, and T. S. Jones[a)]
Ultrafast Photonics Collaboration, Centre for Electronic Materials and Devices, Imperial College London, SW7 2AZ, United Kingdom

(Received 3 November 2003; accepted 10 December 2003)

Atomic force microscopy and photoluminescence spectroscopy (PL) have been used to study asymmetric bilayer InAs quantum dot (QD) structures grown by molecular-beam epitaxy on GaAs(001) substrates. The two QD layers were separated by a GaAs spacer layer (SL) of varying thickness and were grown at different substrate temperatures. Grown independently, these two layers would exhibit a widely different QD number density, and this technique therefore enables us to assess the influence of the strain fields created by the dots in the first layer on the second-layer QD nucleation and characteristics. For very large SLs (>40 nm), total strain relief causes the QD nucleation to be controlled exclusively by the substrate temperature, which influences the migration of In adatoms. In this case, the optical and morphological properties of the second QD layer are identical to a structure with a single QD layer grown at the same temperature. In structures with a much smaller SL, strain effects dominate over the effect of temperature in controlling the nucleation of the QDs, thereby fixing the second-layer QD number density to that of the first (templating effect). There is also evidence that strain relaxation is present in the QDs of the second layer and that this is crucial for extending their emission wavelength. The optimum SL thickness is shown to be 11 nm, for which low-temperature PL emission peaks at 1.26 μm, with a full width at half-maximum of only 15 meV. Intermediate SL thicknesses exhibit broad QD size distributions, with strain effects only partly influencing the QD growth in the second layer. © *2004 American Institute of Physics.* [DOI: 10.1063/1.1645637]

I. INTRODUCTION

Considerable effort has been devoted to studying the growth and properties of InAs/GaAs quantum dots (QDs), with significant progress made in producing optoelectronic devices for applications at ~1.3 μm.[1] More recently, attempts have focused on producing InAs/GaAs QD emitters for longer wavelengths,[2–4] with the ultimate aim of developing GaAs-based QD devices for applications at the technologically important wavelength of 1.55 μm. Emission at longer wavelengths is difficult to achieve when using a single layer of InAs/GaAs QDs; however, we have shown that it is possible to fabricate asymmetric bilayer QD structures that demonstrate room-temperature (RT) emission at wavelengths greater than 1.3 μm.[4] Bilayer QD structures were grown at low InAs growth rates, and through careful control of the second QD layer growth and capping temperature, RT emission at 1.4 μm using only GaAs in the barrier layer was demonstrated. This was extended to ~1.5 μm by including an InGaAs capping layer.[4] For these structures, a remarkably small linewidth of ~14 meV (10 K) was measured, consistent with a narrow distribution of QD sizes and composition.

The ability of this bilayer QD structure to achieve long-wavelength emission depends crucially on being able to exploit the strain fields associated with the first (seed) QD layer. It is well documented from cross-sectional imaging techniques that vertical self-alignment of QDs occurs if the thickness of the spacer layer (SL) is $\leqslant$20 nm.[5–8] This stacking behavior has been attributed to strain interactions.[5,9] The effects of strain and SL morphology on the growth and optical properties of multilayer QDs have also been studied.[10–14] However, most of these studies relate to structures in which each QD layer is grown under nominally identical conditions and the number density of QDs in each layer is essentially the same. This is very different from the case of the bilayer structures developed for long-wavelength emission,[4] in which the two QD layers need to be grown at different temperatures, with strain interactions from the first layer fixing the second layer QD density. Such asymmetric bilayer structures have not been studied in detail so far.[4,6]

In this article, we address the important issue of SL thickness (S) in these asymmetric structures and investigate the effect of the strain fields from the QDs in the first layer on the nucleation, and the structural and optical properties of QDs in the second layer. For that purpose, we measured the size, density, and uniformity of the (uncapped) QDs in the second layer using atomic force microscopy (AFM), while the QD emission properties were characterized by photoluminescence (PL) spectroscopy. It is shown that strain fields can affect the QD nucleation for relatively large SLs, up to at least 30 nm. For SLs between 9 and 18 nm, nucleation is shown to be exclusively driven by the strain field from the first layer, leading to a fixed QD number density, improved size uniformity, and longer-wavelength emission.

[a)]Electronic mail: t.jones@imperial.ac.uk

For applications such as lasers, this study enables us to identify an optimum SL thickness of 11 nm, for which the inhomogeneous broadening of the emission reaches a minimum while long-wavelength emission (1.26 μm at 10 K) is achieved. The changes induced by varying the SL thicknesses are explained in terms of the strain fields that are created by the first-layer dots and that penetrate the GaAs SL.

II. EXPERIMENTAL DETAILS

The samples were grown in a molecular-beam epitaxy (MBE) system equipped with reflection high-energy electron diffraction (RHEED) for *in situ* monitoring of the growth process; in particular, measuring the critical thickness for QD formation (θ_{crit}) and calibration of the incident Ga, In, and As_2 fluxes. Epiready GaAs (001) substrates (n^+ Si-doped) were mounted on molybdenum plates and the samples introduced into the MBE chamber via a fast entry lock. After initial thermal degassing at 300 °C under an As_2 flux (As pressure$=2.6\times10^{-6}$ mbar), the oxide layer was removed at 620 °C and a 200 nm GaAs buffer layer was then grown at 580 °C at a growth rate of 0.5 monolayers per second (ML s^{-1}). The substrate temperature was then reduced for the growth of the InAs/GaAs QDs.

The basic bilayer structure comprised two layers of InAs QDs separated by a GaAs SL of varying thickness *S*. The InAs deposition rate in all cases was 0.016 ML s^{-1}, and 2.5 ML of InAs were deposited in the first layer at 510 °C. The critical coverage for QD formation as measured by RHEED was 2.0 ML. The GaAs spacer layer was also grown at 510 °C and then annealed under an As_2 flux at 580 °C. This annealing process has previously been shown to remove surface undulations that can affect the properties of the QDs in the second layer.[11,12] The critical coverage for second-layer QD formation is the same whether the SL is annealed or not, and is generally (depending on the value of *S*) lower than that of the first layer.[11,14] After annealing, the temperature was reduced to 475 °C before deposition of 2.5 ML InAs for the formation of the second layer of QDs.

Samples for *ex situ* AFM analysis were then removed quickly from the growth chamber (''quenched'') in order to avoid any post-growth annealing processes that are known to alter the morphological QD characteristics.[15] Samples for optical studies were capped with GaAs at the low growth temperature (~475 °C) with an initial 15 nm GaAs layer. The temperature was then raised to 580 °C and a final GaAs capping layer of 90 nm was grown. PL measurements were made using an Ar^+ laser dispersing the light with a SPEX 0.5 m monochromator, and spectra were detected with a cooled Ge diode using standard lock-in techniques.

III. RESULTS AND DISCUSSION

A. Morphological properties

The key issue for the growth of long-wavelength bilayer structures is the templating effect of the seeded (first) QD layer, which dictates the QD number density ($N_{D,2}$) in the second layer,[4,6] provided an appropriate value of *S* is chosen. Due to the strain fields produced by the dots in the first layer, the lattice constant of the GaAs surface is expanded directly above a buried dot,[5] leading to a strain-energy modulation on the surface of the SL. This strongly influences the growth and properties of the second-layer QDs, and under the right conditions leads to a perfect vertical alignment of the QDs in the second layer with those of the first. This templating effect has two advantages. Firstly, it leads to more strain-relaxed QDs in the second layer, which should contribute to a longer-wavelength emission.[4] Secondly, it allows us to choose the growth temperature of the second layer without affecting $N_{D,2}$. In the case of a single QD layer, a reduction in substrate temperature would lead to a substantial increase in dot density,[16] because the migration length of In adatoms is reduced. In a QD bilayer with a suitable SL, the surface diffusion of In adatoms is directed to areas with a lattice constant that is increased compared to that of unstrained GaAs. Nucleation is then exclusively controlled by the strain fields and $N_{D,2}$ is fixed by the first-layer density, independent of growth temperature.

The low substrate temperature for the growth of the second QD layer (475 °C) is a crucial feature for several reasons. Firstly, from an applications point of view, the low growth temperature contributes to the long-wavelength emission, and this has been attributed to the increased QD size and aspect ratio (defined by height over diameter), and to the reduced degree of In/Ga intermixing during capping.[4] Secondly, it provides an indirect tool for measuring the decay of the strain fields over large SLs. The density and morphology of the QDs in the second layer are determined by the balance between strain-induced nucleation and temperature-controlled In-adatom mobility. In the following, we aim to study this balance by investigating the second-layer QD morphology and density as a function of SL thickness *S*.

An AFM image for the uncapped single layer of QDs grown with 2.5 ML of InAs at 475 °C is shown in Fig. 1. The total QD density is 7.5×10^{10} cm^{-2}, and the average height (*h*) and diameter (*d*) are 3.4 and 27.2 nm, respectively. These are typical values for single-layer InAs/GaAs QDs grown under these conditions. As a comparison, a single layer of QDs grown at a substrate temperature of 510 °C exhibits a reduced number density of $\sim1.5-2\times10^{10}$ cm^{-2} (not shown here).[11]

Figures 1(b)–1(e) show AFM images for the uncapped second QD layer of the bilayer structures, consisting of 2.5 ML of InAs deposited at 475 °C after a spacer layer of $S=10$ (b), 20 (c), 30 (d), and 50 (e) nm. Significant changes in QD density ($N_{D,2}$) and size are clearly visible with varying *S*. The small dots seen in image (a) can be easily distinguished from the large ones of image (b). In the case of a single layer, almost all dots have a height of less than 5 nm, whereas in the bilayer structure with $S=10$ nm, only dots with $h>5$ nm exist. For $S=20$ and 30 nm, both classes of dots coexist, while the case $S=50$ nm (e) is similar to the single layer (a) with only small dots. The variation of the density ($N_{D,2}$) of the small ($h<5$ nm) and large ($h>5$ nm) QDs and of the total QD density with *S* is summarized in Fig. 2.

On the basis of QD density and size, it is clear that the influence of the (vertical) strain fields extends up to at least

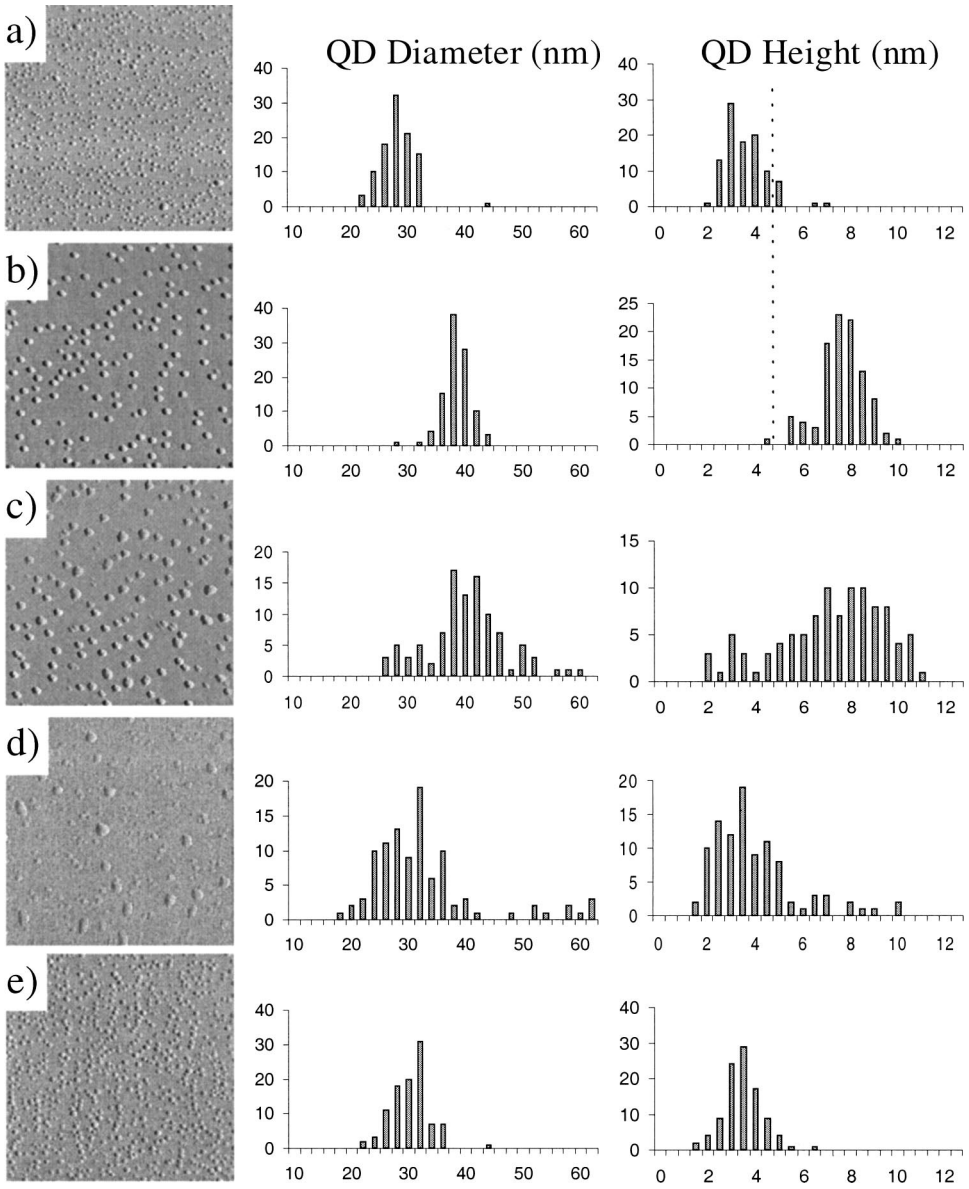

FIG. 1. Contact-mode AFM images (1×1 μm^2) of uncapped InAs/GaAs QD samples. (a) A single QD layer. (b), (c), (d), and (e) The second QD layer with $S=10$, 20, 30, and 50 nm, respectively. Histograms of the measured QD heights and diameters are also shown. The dashed vertical line in the first two height histograms denotes the distinction between small and large dots (see Fig. 2). In all cases, 2.5 ML of InAs were deposited at 475 °C.

30 nm, and it is only for relatively thick SLs ($S>40$ nm) that the properties of the second-layer QDs become similar to those of the first layer when grown under nominally identical conditions. Under these conditions, we conclude that the strain is relieved and therefore the substrate temperature exclusively controls the nucleation of QDs.

For $S\sim10$ nm [Fig. 1(b)], the QD density is similar to that of the first layer. We deduce that there is a perfect vertical alignment for this SL, despite the reduced substrate temperature of the second layer, and the resulting decrease in surface In adatom diffusion. In this regime, strain-induced QD nucleation completely dominates over the effect of a reduced temperature on the In adatom diffusion length. The other striking difference is that only large QDs are observed with average height and diameter of 7.3 and 37.4 nm, respectively. This increase in size is a direct consequence of the strain-induced vertical alignment. RHEED measurements show an earlier two- to three-dimensional (2D–3D) transition ($\theta_{crit,2}$ is reduced; see Fig. 3); consequently, more InAs is incorporated into the QDs and the thickness of the wetting layer is reduced. In addition, due to the lower density [reduced by a factor of around 5 compared to Figs. 1(a) or 1(e)], the average QD volume is increased accordingly. It is also interesting to note that these large QDs have a relatively large average aspect ratio (height over diameter) of 1/5.2, as opposed to 1/9 for the smaller QDs of Figs. 1(a) and 1(e).

For intermediate SLs ($S=20$ or 30 nm), the influence of the strain fields is reduced, and the strain-energy modulation on the surface of the GaAs SL becomes less pronounced as S increases, and eventually disappears for $S=50$ nm. During this transition, QD formation can be strain-induced in some regions where the strain fields from the first layer QDs are stronger, but in others it occurs as if no strain was present. In these latter regions, the low substrate temperature dominates

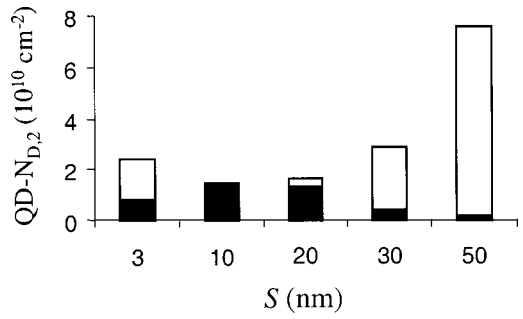

FIG. 2. Plots of the second-layer QD density ($N_{D,2}$) as a function of S. The total height of each column corresponds to the total number density. The heights of the (lower) black part of the columns correspond to large ($h > 5$ nm) dots, whereas the remainder of each column (white) denotes the number density of dots with $h < 5$ nm.

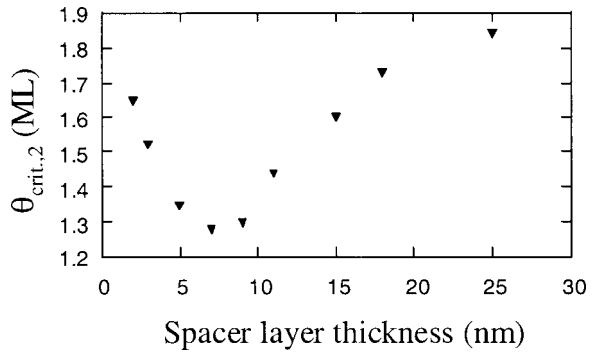

FIG. 3. Critical thickness for the formation of QDs in the second layer ($\theta_{crit,2}$) as a function of GaAs SL thickness as measured by RHEED. For large S, the critical thickness asymptotically approaches the value for a single QD layer (~1.9 ML) grown at the same temperature (475 °C).

over the effects of strain, leading to the formation of relatively small dots due to the reduced surface diffusion of In adatoms. This effect starts to be observed from $S = 20$ nm. The majority of QDs remain large (strain-induced) dots, but one can also observe regions containing a few small QDs [see Fig. 1(c)]. The small reduction in the density of large QDs (Fig. 2) indicates that these regions probably lie above a relatively small QD in the first layer, whose strain field was not strong enough to extend throughout the spacer. At $S = 30$ nm [Fig. 1(d)], the situation is reversed, with only a few regions where nucleation is influenced by the strain field from a—possibly larger than average—dot in the first layer. Strain-induced nucleation then dominates only locally over temperature effects to form a large QD. In other regions, the temperature controls QD formation, resulting in a high density of smaller QDs.

Figure 1 also shows the distribution of QD height and diameter for each case. These distributions can be fitted with a Gaussian for the case of Figs. 1(a), 1(b), and 1(e), and are characterized by σ, the ratio of the full width at half-maximum (FWHM) and the average value (in percent). As expected, the size distributions for the second-layer QDs grown with $S = 50$ nm ($\sigma_D = 11.9\%$; $\sigma_H = 24.7\%$) are comparable to those obtained for the single layer ($\sigma_D = 10.9\%$; $\sigma_H = 25.1\%$). A much narrower size distribution is obtained for $S = 10$ nm (diameter, $\sigma_D = 6.4\%$; height, $\sigma_H = 14.6\%$). This is consistent with previous studies, which showed enhanced uniformity in stacked QD layers,[4,6,13] and with the PL results presented in Sec. B.

For $S = 20$ and 30 nm, the distribution cannot be fitted with one Gaussian because of the presence of two types of QDs (strain-induced large QDs and small QDs). It is, however, clear from Figs. 1(c) and 1(d) that the individual distribution of each population is much broader than that observed in Fig. 1(a) for small QDs and Fig. 1(b) for large QDs, respectively. We attribute this to the competition between the temperature (diffusion)-controlled and strain-induced QD nucleation processes. For intermediate SLs, neither process dominates. Therefore, each is influenced by the other, and this introduces a new source of size fluctuations for each population of dots. This is evident in Fig. 1(c), where the distribution of large strain-induced QDs is broadened compared to 1(b), and in Fig. 1(d), where the distribution of small QDs is broadened compared to 1(e).

Finally, for very small SL thickness ($S = 3$ nm not shown here), the QD characteristics are comparable with those of intermediate SLs ($S = 20$ or 30 nm). At first glance, this result is surprising since the strain effects should be much more pronounced at very low values of S. However, the high-temperature annealing (580 °C) of the sample after growth of the GaAs SL and prior to second-layer InAs deposition leads to In segregation through the thin SL and subsequent desorption of In from the surface. This effectively reduces the size of the buried first layer QDs, and consequently the associated strain fields are significantly reduced. This is apparent in Fig. 3, which shows the thickness of the wetting layer at the 2D–3D growth-mode change in the second layer as a function of SL thickness. The transition thickness is reduced compared to the value of the first QD layer as S is decreased due to the strain fields. However, it increases again as S is reduced from 7 to 2 nm, indicating a reduction in the strength of the strain fields. A more detailed analysis of segregation effects for thin SLs will be presented elsewhere.

The best uniformity is therefore achieved when strain-induced nucleation completely dominates over temperature effects; it is lost at small and large SL thicknesses. An optimum SL thickness must therefore exist for optimum QD uniformity, and it is important for applications to determine whether this translates into good optical properties. Section B presents the results of a study of the optical properties of these QD bilayers. Combined with the structural properties, we can gain more insight into the nature of the strain effects.

B. Optical properties

The effects of varying S on the emission properties of the bilayer QD structures can be seen in Fig. 4, which shows examples of normalized, low-temperature (10 K) PL spectra, recorded at low excitation density (0.1 W cm^{-2}) to avoid emission from the excited states of the QDs. In the spectrum with $S = 18$ nm, two peaks are seen at 1.26 and ~1.14 μm, respectively. The peak at 1.14 μm is attributed to ground state (GS) emission from the first QD layer, since it is very similar to the emission spectrum of a single layer grown identical to the first layer (see later). The long-wavelength

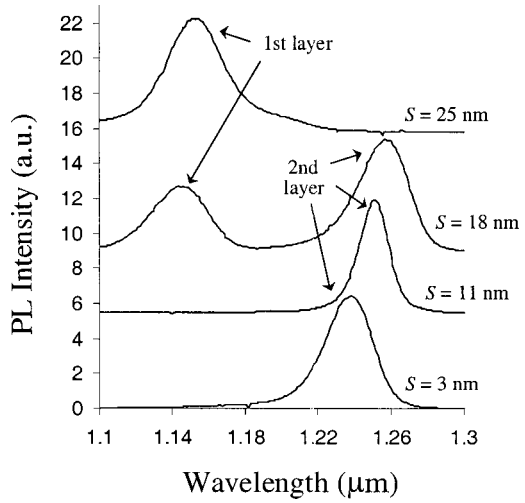

FIG. 4. Low-temperature (10 K) PL spectra for four InAs/GaAs QD bilayer samples, separated by a GaAs SL of varying thickness *S*. The excitation density is very low ($\sim 0.1\ \mathrm{W\,cm^{-2}}$) to avoid emission from the excited states. The peaks at long wavelengths can be attributed to emission from the GS of the dots from the second layer. The spectra are normalized and vertically displaced.

peak at 1.26 μm is attributed to emission from the second layer QDs. This has been verified by using a variable pump wavelength technique which utilizes a He/Ne laser instead of the Ar^+ laser for optical pumping, in order to assign unambiguously each peak to each layer.[17] As *S* is reduced, the low-energy peak (second layer) remains essentially at the same wavelength for $S=11$ nm, and shifts slightly to $\sim$1.24 μm for $S=3$ nm. In addition, it can be seen that the linewidth of the emission is significantly less for $S=11$ nm compared with $S=3$ and 18 nm. Moreover, emission from the first QD layer is absent for small SLs (less than 15 nm due to carrier tunneling between QDs of each layer).[12] For these small barrier thicknesses, tunneling is much faster than the radiative lifetime of the carriers in the GS of the QDs in the first layer. Carriers therefore tunnel rapidly to an excited state of a QD in the second layer, from where they relax to the GS. Only emission from the GS in the second layer is then observed.[12,18] However, by using high excitation density emission from the first layer, dots can be seen despite the high tunneling rates. In this case, a peak at 1.14 μm appears for the sample with $S=11$ nm, and for $S=3$ nm, the (first layer) peak appears at $\sim$1.1 μm. This blueshift may reflect the decreased dimensions of the QDs in the first layer, and confirms the assumptions made in Sec. A about In desorption during sample annealing when they are protected by only very thin SLs.

In the sample with $S=25$ nm, only one relatively broad emission peak is present, with a maximum at 1.15 μm. This is also the emission wavelength obtained for a single layer of QDs grown at 475 °C (and therefore having a high density of small QDs). We conclude that this peak is a superposition of emission from the first layer around 1.14 μm and from small dots in the second layer around 1.15 μm. This is consistent with the AFM study that shows that a large number of small dots are present for such a SL thickness. However, this study showed that a number of large dots (similar to those observed for $S=11$ nm) should also be present, and one would expect to observe emission from them at a longer wavelength. In fact, there is a low-energy shoulder in the emission peak centered around 1.2 μm, which we attribute to these large QDs. However, this peak is strongly blueshifted compared to the emission at 1.26 μm observed for $S=11$ or 18 nm. Long-wavelength emission from the second layer was previously attributed to several factors.[4] Firstly, the low growth temperature leads to an increased aspect ratio of the QDs (and therefore increased height) and a reduction of In/Ga intermixing during capping. It was also proposed that the strain relaxation could be preserved in the QDs during GaAs capping and could also contribute to the longer-wavelength (owing to the strain-induced redshift of the bandgap of InAs). Such a strain relaxation has recently been evidenced in buried, closely stacked InAs QDs.[8,19] This latter factor is the only one that could contribute to the difference in emission wavelength between the large dots of $S=25$ nm and those of $S=11$ nm, since growth temperature and average height are the same. The observed blueshift of the large dots for $S=25$ nm is therefore attributed to the much weaker strain fields they experience from the first layer. The strain is strong enough to induce nucleation of some QDs, as discussed in Sec. A, but is too weak to preserve a strain-relaxed state in the QDs after capping with GaAs. This observation confirms that the strain field from the first layer is not only important for the templating effect, but also contributes to the long-wavelength emission.

An independent confirmation of the presence of strain fields on the surface of the SL can be gained from the PL emission from QDs in which growth is stopped after deposition of the GaAs spacer. It has already been shown that the PL emission from partially capped QDs was strongly redshifted with respect to the same QDs buried below a large GaAs cap.[20] This was explained by a larger strain relaxation (more InAs-like lattice constant) in the partially capped QDs, which is then lost when larger GaAs cap layers are grown. The growth of the GaAs cap layer effectively compresses the QDs and the surrounding GaAs back to the GaAs lattice constant, but this compression effect is not complete until a sufficiently thick layer of GaAs is deposited. When this thickness is reached, it is reasonable to assume that the strain fields from the QDs no longer extend through the SL up to the surface; otherwise, the deposition of more GaAs would result in more compression. As shown in Fig. 5, this effect can be probed by measuring the PL emission of the first QD layer capped with only a thin GaAs SL of thickness *S*, and by comparing it to that obtained for a large capping layer (here, 100 nm). A redshift of the PL emission is observed for $S=10$ nm, and is a direct consequence of the more strain-relaxed state of the QDs because the GaAs compression effect is not complete. We emphasize that this redshift, which was previously reported for partially capped QDs,[20] occurs here for fully capped QDs and is a result of strain relaxation because the GaAs cap is not thick enough to fully compress the dots. The redshift is also accompanied by a large increase of the FWHM (from 35 to 70 meV). This can be understood since strain relaxation brings a new source of fluctuations that is not present when all the QDs are fully strained (as in

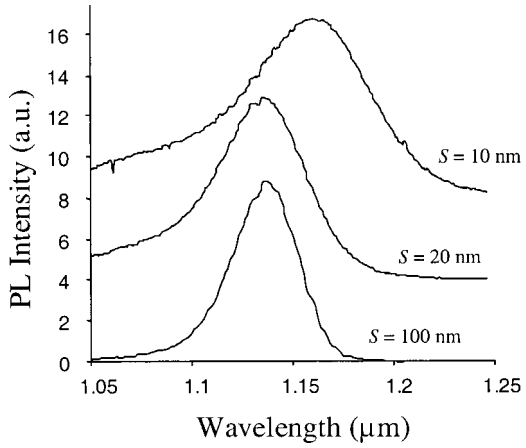

FIG. 5. PL spectra, recorded at 10 K of the first QD layer capped with GaAs thicknesses of 10, 20, and 100 nm. The PL intensities (which are much lower for thinner caps) have been normalized and the spectra vertically displaced for easier comparison.

the lower spectrum of Fig. 5). For $S=20$ nm, the redshift is no longer detectable, but the FWHM (of 50 meV) remains larger than that for large caps, indicating that the dots are still partially strain relaxed. These results therefore confirm two of our previous conclusions: strain relaxation in the QDs can affect the PL emission, and the strain fields extend through relatively large SLs (here at least 20 nm).

More detailed information regarding the PL emission properties of the second QD layer is also summarized in Fig. 6, which shows plots of the wavelength and linewidth (FWHM) as a function of *S*. The emission wavelength remains essentially constant in the range $9\text{ nm} \leqslant S \leqslant 18\text{ nm}$. Such behavior is difficult to explain since the intensity of the strain field is expected to vary widely over this range of SL

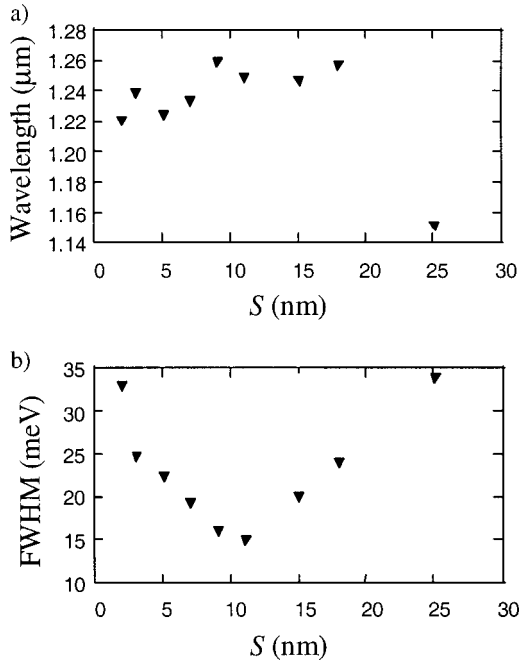

FIG. 6. Emission wavelength (a) and FWHM (b) as a function of *S* for a series of InAs/GaAs bilayer QD samples.

thicknesses. We have just shown that a strong strain field contributes to the long wavelength through strain relaxation of the QDs in the second layer. The intensity of the strain field can be monitored by the reduction of the critical thickness in the second layer (using RHEED), which is maximum for $S=7$ nm (see Fig. 3). As mentioned in Sec. A, the strain field eventually becomes smaller for very small SLs due to In desorption during annealing of the SL, but this is only apparent for $S<7$ nm. We would therefore expect the wavelength to redshift continuously from $S=18$ to 7 nm, as the strain fields become stronger and consequently the strain relaxation in the second-layer dots is larger. As this is not the case, another mechanism that compensates this expected redshift must be operating. It is already known that strain relaxation induces intermixing during capping,[10,11] especially at high substrate temperatures, and this was thought to be strongly reduced or even absent at 475 °C. We propose that for the largest strain field, a temperature of 475 °C may still not be low enough to prevent all intermixing effects, and this could compensate the redshift that is expected from the larger strain relaxation. This would explain why the emission wavelength remains constant between $S=18$ and 9 nm, and why it even decreases slightly for 7 nm, for which the effect of strain-induced intermixing probably dominates over the strain-relaxation effect on the wavelength. To support this hypothesis, the same sample was grown with a substrate temperature of only 460 °C in the second layer. The wavelength then increases to 1.255 μm, confirming that intermixing effects were still present at 475 °C.

More pronounced changes occur in the inhomogeneous broadening of the emission, as shown in Fig. 6(b). We mentioned in Sec. A that the size distribution of the QDs should exhibit maximum uniformity for some SL thickness. This translates into a minimum in the FWHM of only 15 meV observed for $S=11$ nm. This SL is therefore the optimum value for applications such as lasers, for which a narrow linewidth is desirable to maximize the modal gain. It also presents the following advantages: firstly, because tunneling is fast between the two layers, most carriers will be efficiently channeled to the second layer (which is the active layer for applications); and secondly, the RT emission wavelength of the first excited state of the second layer is close to 1.3 μm, and this structure could thus enable the realization of lasers operating at 1.3 μm from the first excited state of the QDs, for which the saturated modal gain is twice as large as for the ground state.

IV. SUMMARY

The influence of the spacer layer thickness on the density, size, and optical properties of asymmetric bilayer InAs/GaAs QD structures has been investigated. Different regimes have been identified for which nucleation is controlled either exclusively by the strain field from the first layer or by the substrate temperature, and its influence on the diffusion of In adatoms. Intermediate regimes have also been identified for intermediate or very small SL thicknesses, and were shown to lead to wider size distributions. Total strain relief is shown to occur only for relatively large SL thicknesses (larger than

40 nm), and this has implications for the growth of multilayer samples necessary for many applications. It was also shown that, despite a reduced substrate temperature, the number density of QDs in the second layer can be fixed to that of the first layer, provided an appropriate thickness is chosen for the GaAs SL. The optimum size uniformity is observed for a SL thickness of around 11 nm, and this translates into a narrow emission at a long wavelength. Finally, this study confirms the importance of strain relaxation in the realization of long-wavelength QDs and furthermore, that strain engineering of InAs/GaAs QDs is a highly promising technique for the realization of 1.55 μm optoelectronic devices on GaAs substrates.

ACKNOWLEDGMENTS

This work was supported by the EPRSC, UK, who also provided studentships for three of the authors (P. H., E. C., and B. A.).

[1] V. M. Ustinov and A. E. Zhukov, Semicond. Sci. Technol. **15**, R41 (2000), and references therein.
[2] K. Nishi, H. Saito, S. Sugou, and J.-S. Lee, Appl. Phys. Lett. **74**, 1111 (1999).
[3] J. Tatebayashi, M. Nishioka, and Y. Arakawa, Appl. Phys. Lett. **78**, 3469 (2001).
[4] E. C. Le Ru, P. Howe, T. S. Jones, and R. Murray, Phys. Rev. B **67**, 165303 (2003).
[5] Q. Xie, A. Madhukar, P. Chen, and N. P. Kobayashi, Phys. Rev. Lett. **75**, 2542 (1995).
[6] I. Mukhametzanov, R. Heitz, J. Zeng, P. Cheng, and A. Madhukar, Appl. Phys. Lett. **73**, 1841 (1998).
[7] B. Lita, R. S. Goldman, J. D. Philips, and P. K. Battacharya, Appl. Phys. Lett. **74**, 2824 (1999).
[8] D. M. Bruls, P. M. Koenraad, H. W. M. Salemink, J. H. Wolter, M. Hopkinson, and M. S. Skolnik, Appl. Phys. Lett. **82**, 3758 (2003).
[9] J. Tersoff, C. Teichert, and M. G. Lagally, Phys. Rev. Lett. **76**, 1675 (1996).
[10] M. O. Lipinski, H. Schuler, O. G. Schmidt, K. Eberl, and N. Y. Jin-Phillip, Appl. Phys. Lett. **77**, 1789 (2000).
[11] P. B. Joyce, E. C. Le Ru, T. J. Krzyzewski, G. R. Bell, R. Murray, and T. S. Jones, Phys. Rev. B **66**, 075315 (2002).
[12] E. C. Le Ru, A. J. Bennett, C. Roberts, and R. Murray, J. Appl. Phys. **91**, 1365 (2002).
[13] H. Heidemeyer, S. Kiravittaya, C. Müller, N. Y. Jin-Philipp, and O. Schmidt, Appl. Phys. Lett. **80**, 1544 (2002).
[14] P. B. Joyce, T. J. Krzyzewski, P. H. Steans, G. R. Bell, J. H. Neave, and T. S. Jones, J. Cryst. Growth **244**, 39 (2002).
[15] J.-J. Shen, A. S. Brown, R. A. Metzger, B. Sievers, L. Bottomley, P. Eckert, and W. B. Carter, J. Vac. Sci. Technol. B **16**, 1326 (1998).
[16] P. B. Joyce, T. J. Krzyzewski, G. R. Bell, B. A. Joyce, and T. S. Jones, Phys. Rev. B **58**, 15981 (1998).
[17] E. C. Le Ru, U. Marchioni, A. Bennett, P. B. Joyce, T. S. Jones, and R. Murray, Mater. Sci. Eng., B **88**, 164 (2002).
[18] R. Heitz, I. Mukhametzanov, P. Cheng, and A. Madhukar, Phys. Rev. B **58**, 10151 (1998).
[19] J. Ibáñez, A. Patanè, M. Henini, L. Eaves, S. Hernández, R. Cuscó, L. Artús, Yu. G. Musikhin, and P. N. Brounkov, Appl. Phys. Lett. **83**, 3069 (2003).
[20] H. Saito, K. Nishi, and S. Sugou, Appl. Phys. Lett. **73**, 2742 (1998).